Feasibility of spent macroalgae biochar for removal of Acid Red 88 (AR) dye from its aqueous solution

Thinakaran E.[1]*, Brema J.[2], and Arumairaj P.D.[3]

[1]Research Scholar, Department of Civil Engineering, Karunya Institute of Technology and Sciences (Deemed University), Coimbatore

[2]Professor, Department of Civil Engineering, Karunya Institute of Technology and Sciences (Deemed University), Coimbatore

[3]Managing Director, Alzum Geocivil Integrated Services, Coimbatore

*to whom all correspondence should be addressed: e-mail: thinakaranmumbai@gmail.com

Graphical abstract

Abstract

Biochar was synthesized from *Kappaphycus alvarezii* reject (KR) remove the anionic azo dye, Acid Red 88 from wastewater. In this study, biochar was experimented in both batch and column adsorption studies. Batch adsorption studies were performed at varying temperature (25 – 40 °C), dosage (1 – 10 g), pH (4 – 10), time (30 – 90 min) and dye concentration (25 – 125 mg/L) respectively. From the batch adscorption studies, it was seen that maximum removal efficiency was 87.64% at 75ppm, dosage of 4 g/L, time of 60 min and pH 7 respectively. The batch adsorption experiment best fitted to Freundlich isotherm model with Pseudo-second-order kinetics indicating the adsorption to follow chemisorption mechanism process along with multilayer adsorption onto biochar's uneven adsorption sites. It was clear from this study, that *Kappaphycus alvarezii* reject has the potential to serve as economical biochar as it can be utilized as an adsorbent for the efficient removal of colorants from wastewater.

Keywords: Adsorption, macroalgae, acid red, wastewater

1. Introduction

One of the major issues that we are facing now is the pollution of soil, air and water bodies. The first most crucial is air pollution as it is causing serious climate change and imminent global warming. Nowadays, with increasing industrialization and the requirement to meet human needs, water pollution is also becoming a major concern. Water pollution usually occurs when industries do not treat their effluents before letting them out into the environment. Many pollutants such as heavy metals, pharmaceutical compounds, organic substances, pesticides, chemicals and more importantly, dyes. Dye pollution is of major concern as the majority of the industry utilizes dye in one form or the other and are not keen on treating its effluent for the removal of dyes (Jayaraju *et al.*, 2021; Gokulan *et al.*, 2018; Sivarethinamohan *et al.*, 2021). Amongst these industries, the textile industry is the industry that utilizes a tremendous quantity of water and dyes in their process and let out wastewater containing a huge amount of untreated dye and other chemicals. These chemicals include surfactants, dyes, minerals, recalcitrant, solvent, heavy metals, electrolytes and biocides. It has been estimated that about 5 – 50% of the dyes and chemicals utilized in the textile industries are let out into the environment without proper treatment and the annual discharge of dye into wastewater effluent is about 280,000 tons (Vickers, 2017). These dyes that are let into the environment are not only complex in their structure, hindering the ease of removing them but are also carcinogenic when containing azo or phthalocyanine chromophores in them. Owing to their harmful nature, not only to the aquatic ecosystem but also to humans, the removal of such dyes from the environment is essential (Rao *et al.*, 2021).

Generally, the organic materials obtained from animals or plants including their waste by-products are collectively called biomass (Gokulan *et al.*, 2019; Sundar *et al.*, 2021; Kalyani *et al.*, 2021). Biomass is divided into three categories based on the source from which they are

obtained. Biomass obtained from land are called terrestrial biomass and this includes substance such as grasses, crops, etc. Biomass obtained from the aquatic system is called aquatic biomass and this includes micro and macroalgae, marine plants, etc. And the last one is the waste biomass meaning that they are obtained from the waste by-products of terrestrial and aquatic biomass. Such type of waste biomass is only utilized in our study. *Kappaphycus alvarezii* is a macroalga cultivated in seashores for its application in cosmetics, food, medicine, etc. After extracting essential substances for the production of fertilizers, carrageenan and agar from the macroalgal biomass, the by-product waste obtained is called the reject. The reject is usually fibrous and found to be rich in energy (Ravindiran *et al.*, 2021).

As biomass is rich in energy, it is wise to utilize them as they are a waste and utilizing them will not only reduce the waste but also help in the production of the more valuable substance. For such conversion of waste biomass into a valuable product, we utilize economical and efficient thermos-chemical conversion processes such as hydrothermal liquefaction, pyrolysis, hydrothermal carbonization, torrefaction, combustion and gasification. Amongst all these thermos-chemical processes, the best process can be selected only based on two factors: 1) Type of Biomass and 2) Desired Product (Ramirez, 2017; Basu, 2018; Vassilev *et al.*, 2010; Wang *et al.*, 2018; Jegatheesan *et al.*, 2016). As we are required to produce biochar for utilizing it as an adsorbent of dye removal, the best thermos-chemical conversion process for this study is the hydrothermal carbonization process. The reason for considering HTC as a better fit for this study than the other thermos-chemical conversion process is due to the following properties of HTC over other processes: 1) Highly energy-intense drying process is not required, 2) Operates at a relatively lower temperature and residence time and 3) Removes inorganic substances. The HTC process not only converts the wet biomass into useful biochar but also helps in recovering organic nutrients as the product of HTC are 1) Hydrochar and 2) Organic nutrients rich processed water (Kumar *et al.*, 2021; Praveen *et al.*, 2021; Saravanan *et al.*).

Many studies have been conducted to examine the ability and effectiveness of biochar to remove colours from wastewater due to its intrinsic qualities such as being rich in carbon, dense in energy, and so on. However, the vast majority of these biochars were made from terrestrial or aquatic biomass, as well as waste biomass such as municipal and sewage effluent in some situations. Only a few studies exist on the use of macroalgal refuse for the synthesis of biochar via the HTC process and for the removal of dye. As a result, in this study, we are using a hydrothermal carbonization technique at 350 °C and 5 MPa for 1 h to produce hydrochar from the reject derived from *Kappaphycus alvarezii* macroalgae. Using batch and column adsorption tests, the dye removal efficiency of the biochar is determined. Furthermore, the best operating conditions for the removal of AR dye are identified by adjusting operational factors such as biochar dose,

beginning dye concentration, contact time, temperature, and pH.

2. Material and methods

2.1. Raw material collection, characterization and wastewater preparation

The *Kappaphycus alvarezii* reject (KR) obtained after processing of the *Kappaphycus alvarezii* macroalgae was collected from one of the five coastal districts of Tamil Nadu cultivating this macroalga, Tharuvaikulam, Tuticorin, Tamil Nadu, India. The collected *Kappaphycus alvarezii* reject (KR) was characterized for its physio-chemical properties such as proximate, elemental and biological composition. Furthermore, the Higher Heating Value (HHV) of the KR was calculated using Eq. (1) and its thermal behaviour was studied by applying Thermogravimetric Analysis (TGA). The Acid Red 88 (CAS: 1658-56-6, $C_{20}H_{13}N_2NaO_4S$, 400.4 g/mol) (≥ 90.0% anhydrous basis, Sigma-Aldrich) dye used in this study was purchased from Merk, India. Initially, a 500-ppm stock solution of AR was prepared by dissolving 0.5 g of AR into 1000 mL of distilled water in a conical flask and then the 500-ppm stock solution was diluted as required using distilled water.

$$HHV(MJ/Kg) = 0.338 \times C + 1.428 \times (H - O/8) \quad (1)$$

2.2. Hydrothermal carbonization (HTC) for biochar production

The collected KR was initially washed several times with distilled water to remove the impurities present on them after which it was oven-dried for 1 h at 110 °C. Then, the KR was grounded into smaller particles using a grinder and stored in plastic air-tight containers at room temperature. The HTC process was carried out in an autoclave reactor lined with Teflon under a nitrogen atmosphere, by adding the feedstock and solvent (water) in a biomass-to-solvent ratio of 10 wt%. The process was carried out at a temperature of 350 °C and a pressure of 5 MPa for 1 h. The product obtained after the completion of the HTC process is a mixture of liquid and solid particles of which the solid particle is the biochar, also called hydrochar. After the completion of the reaction, the reactor was allowed to cool down and the products were taken out for the separation process. The hydrochar was separated from the mixture through vacuum filtration. The volatile compounds that might have stuck onto the hydrochar were removed by boiling the hydrochar with distilled water. After which, the hydrochar is washed with distilled water several times and oven-dried for 1 h at 110 °C to ensure complete removal of moisture content (Bhatt *et al.*, 2018; Patel *et al.*, 2016, 2021). This processed biochar is utilized for the batch and column adsorption studies for the removal of AR dye.

2.3. Batch adsorption

The ability of the produced biochar to efficiently remove AR dye was studied in a batch adsorption experiment. The parameters of the adsorption experiments were varied to determine the optimum ones at which we achieve

maximum removal percentage. For this, about 1 – 10 g of biochar was added to a containing 100 mL of 25 – 125 mg/L AR dye solution and the mixture was kept in a shaker for 30 – 90 min at a temperature of 25 – 40 °C and pH of 4 – 10. Initially, one parameter was changed while the others were kept at a constant value determined by considering previous literature (Praveen *et al.*, 2021; Ravindiran *et al.*, 2022). The optimum value of that parameter was found and was updated in the next optimum parameter determining experiment. After the completion of each batch adsorption experiment, the final dye concentration in the mixture was determined using a UV-vis spectrophotometer and the removal percentage was calculated using Eq. (2), Where Co (mg/L) is the initial dye concentration and Ce (mg/L) is the final equilibrium dye concentration.

$$\text{Removal}(\%) = \frac{C_o - C_e}{C_o} \times 100 \tag{2}$$

2.4. Isotherm and kinetics

Adsorption Isotherms are very useful in analyzing the adsorption process as it not only explains the extent to which the adsorbent and adsorbate molecules interact but also helps predict the behaviour of the adsorbent when we change the operating parameters using the model parameters. Similarly, Adsorption kinetics are very important as they help us understand the mechanism and dynamics through which the adsorption occurs. With the help of these data, we will be able to efficiently design an adsorption process. In this study, Langmuir and Freundlich's isotherm models are employed to model the isotherm data and pseudo-first order, pseudo-second order, Weber-Morris, and Elovich kinetic models are employed to model the kinetics data. The equations of the isotherm and kinetics model used in this study are listed in Table 1 (Bhatt *et al.*, 2018; Patel *et al.*, 2016; Li *et al.*, 2018; Sharma *et al.*, 2020). With the help of the Correlation factor (R^2), the perfect fit of isotherm and kinetics models for this study were determined.

Table 1. Isotherm and Kinetics Equation

Isotherm model	
Langmuir	$\dfrac{1}{q_e} = \dfrac{1}{q_e K_L} \cdot \dfrac{1}{C_e} + \dfrac{1}{q_m}$
Freundlich	$\log q_e = \log K_F + \dfrac{1}{n} \log C_e$
Kınetıcs model	
Pseudo-First order	$q_t = q_e \left(1 - exp(-k_1 t)\right)$
Pseudo-Second order	$q_e = \dfrac{q_e^2 k_2 t}{1 + q_e k_2 t}$
Webber-Morris	$q_e = k_p t^{\frac{1}{2}} + C$
Elovich	$q_e = (1 + \beta_E) \times \ln(1 + \alpha_E \beta_E t)$

Abbreviation: q_e (mg/g) – Amount of dye adsorbed at equilibrium; q_m (mg/g) – Amount of dye adsorbed after saturation; C_e (mg/L) – Equilibrium dye concentration; K_L – Langmuir adsorption constant; K_F – Freundlich adsorption constant; n – Freundlich exponent; k_1 (1/h) – Pseudo-first order rate constant; k_2 (g/mg h) – Pseudo-second-order rate constant; α (mg/g h) – Initial adsorption rate; β – Elovich constant; q_t (mg/g) – Adsorption capacity; k_p – Webber-Morris constant; C – Intercept.

2.5. Desorption

Desorption experiments aid in understanding the recovering process of adsorbent and the adsorbate. In addition to this, it also aids in explaining the adsorption mechanism. Desorption studies were conducted to regenerate the spent adsorbent because it makes the treatment process more cost-effective. Here, NaOH, HCl and De-ionized water are utilized as the elutants for the desorption of the adsorbed dye molecules from the biochar surface. The spent biochar (1 g) was added to the elutants (100 mL) in a conical flask (250 mL), mixed for an hour, separated from the mixture and oven-dried to be used for the next adsorption cycle (Ravindiran *et al.*, 2019).

2.6. Column adsorption

In this study, two different beads namely, hybrid beads and encapsulated beads were prepared and studied for their column adsorption efficiency. The bead that has the maximum adsorption efficiency will be utilized for studying the effect of bed height (10, 15, 20, and 25 cm) on the adsorption process using the bed-depth service time (BDST) model. For the column adsorption experiment, we used a glass column apparatus having the following dimensions: Length: 30 cm and Internal Diameter: 3 cm. The column was filled with the best performing bead up to the desired height and glass wool was added to the top and bottom of the glass apparatus as a support to prevent the beads from floating in presence of excess dye wastewater. The dye wastewater was let into the glass apparatus in an upward flow mode continuously through a flow regulated pipe attached to a pump. To determine the dye concentration at regular intervals, the effluent wastewater was sampled accordingly (Gokulan *et al.*, 2019).

3. Results and discussion

3.1. Biomass and biochar characterization

It is important to characterize the biochar in order to compare and contrast the results with the literature. Thus, the obtained biomass and biochar was subjected to several characterization techniques to determine their

composition. The results of the proximate analysis revealed that the KR had a relatively equal and higher percentage of volatile substances (40.75%) and ash content (45.35%). The remaining were moisture (13.24%). The fixed carbon content of KR was found to be 0.66%. After the biomass was subjected to elemental analysis, the percentage of carbon, hydrogen, nitrogen, sulfur and oxygen were found to be 35.86, 7.6, 5.7, 1.3 and 49.54% respectively. The H/C and O/C ratios were also found to be 2.543224 and 1.036113 respectively. On performing the elemental analysis of the biochar which is produced by performing HTC, as expected the carbon content (86.78%) was a little high and nitrogen content (0.7%) was decreased to an extent. While the hydrogen (7.2%) and sulfur (0.6%) were about the same. The biological composition of the biochar was also determined and it was found that mostly it was made of protein (31.25%) and the rest were lipid (24.76%) and carbohydrate (17.36%) majorly. In addition to this, TGA analyses were also performed to uncover its thermal behaviour from 100 to 800 °C and it is depicted in Figure 1. From looking at the trend shown in the graph, it could be deciphered that the moisture content of KR is lost within 200 °C after which the volatile and the organic content is dissipated. At 20 °C/min heating rate, efficient degradation of KR could be seen when compared to other heating rates.
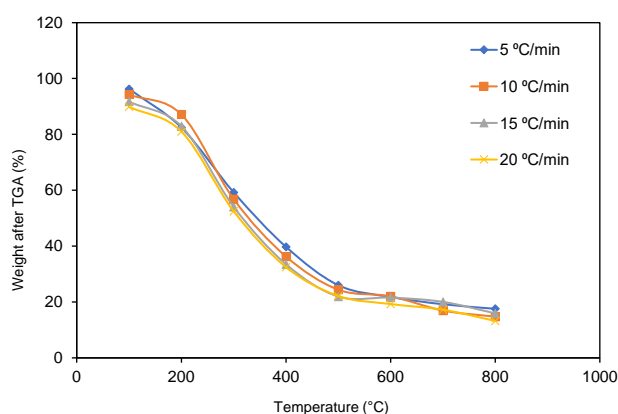

Figure 1. TGA analysis.

3.2. Batch adsorption study

3.2.1. Impact of biochar dosage on removal efficiency

The dosage of biochar is one of the crucial aspects to consider as far as scaling up is concerned. Thus, the apt dosage level must be identified which not only yields better efficacy but also minimal. For these reasons, a batch-wise study was conducted to study the impact of the dosage level of the chosen adsorbent and evaluate its capacity to grab the maximum amount of dye in the solution. Since it is a batch study only ten different dosage levels were adopted to carry out the experiment and find the corresponding removal efficiency. These dosage levels varied from 1 g/L to 10 g/L in steps of one. Other process variables were also set. The amount of dye present before the start of the experiment was about 75 ppm while the pH and temperature were maintained constantly at 7 and 35 °C respectively. After the finishing of the experiment which went for around 60 min, the removal efficiency for

each batch was carefully evaluated and collated against the dosage. This plot could be found in Figure 2. From the illustration, it could be grasped that the removal efficiency of the biochar slowly increases along with the rise in dosage of the biochar. This steady growth in trend might be because of the populated active sites and surface area available on the biochar increasing its potential to adsorb more molecules. Figure 2 reveals that the peak removal occurred at 9 g/L with around 90.507%. Beyond this level, it could be seen that the removal efficiency drops. Since the amount of adsorbent that is introduced into the system is constant while the amount of dye keeps on declining, a gradient in concentration begins to develop inhibiting the adsorbent's ability to adsorb more molecules. With that being said, the optimal dosage level of the biochar must be decided for better performance and economics at the same time. Having discussed all these, the removal efficiency of 87.640% at 4 g/L grabs our attention. This is the only dosage level at which a minimal amount of biochar is used and could remove the maximal dye. The change in percentage from 3 to 4 g/L is also promising when compared to others. Hence 4 g/L of the biochar is considered the best and most efficient dosage level. Similarly, Mahendran *et al.* experimented on the effect of biochar dosage on adsorption efficiency on the removal of Reactive Red 120 using biochar derived from *Ulva prolifera* biomass and found that the removal efficiency of the biochar increased with an increase in the biochar dosage as seen in our study while 2 g/L being their best biochar dosage (Mahendran *et al.*, 2021).
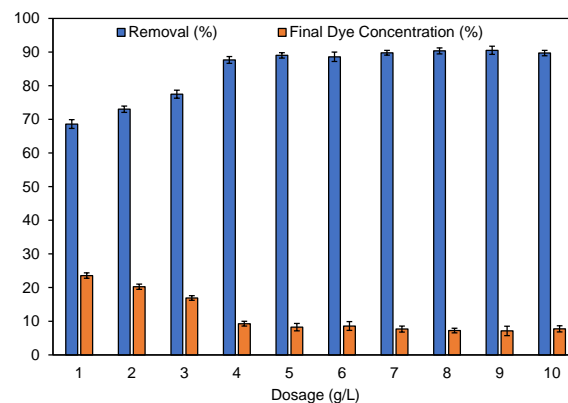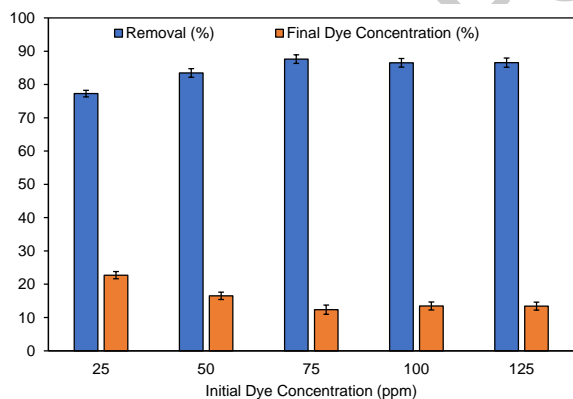

Figure 2. Impact of biochar dosage on removal efficiency.

3.2.2. Impact of Dye's initial concentration on the removal efficiency

The concentration of AR dye before the beginning of the experiment must also be studied for better performance of the adsorbent and to gain more efficient removal. For these reasons, a batch-wise study was conducted to study the impact of initial dye concentration and evaluate its influence on the adsorbent's capacity to grab the maximum amount of dye in the solution. Since it is a batch study only five different concentrations of the dye were adopted to carry out the experiment and find the corresponding removal efficiency. These initial concentration levels varied from 25 to 125 ppm in steps of 25. Other process variables were also set. The dosage level of the biochar as discussed already was set to 4 g/L

while the pH and temperature were maintained constantly at 7 and 35 °C respectively. After the finishing of the experiment which went for around 60 min, the removal efficiency for each batch was carefully evaluated and collated against the process variable i.e., initial concentration of AR dye. This plot could be found in Figure 3. From the illustration, it could be grasped that the removal efficiency of the biochar slowly increases along with the rise in the initial concentration of AR dye. This steady growth in trend might be because of the growing driving force possessed between the dye and adsorbent molecules. Also, the gradient in concentration develops and leads to break the resistance formed by the mass transfer barrier, thus an increase in adsorption takes place. Figure 3 reveals that the peak removal of 87.640% occurred at 75 ppm. Beyond this level, it could be seen that the removal efficiency becomes steady with slight dips. With that being said, the optimal initial concentration level of AR dye must be decided for better performance and economics at the same time. Having discussed all these, the removal efficiency of 87.640% at ppm grabs our attention. The change in percentage from 50 ppm to 75 ppm is also promising when compared to others. Hence 75 ppm of the AR dye is considered the best and most efficient concentration to be set before the starting of the experiment. Similar studies were conducted by Dadebo and Obura in which they experimented on the effect of initial dye concentration on the removal of Acid Red 88 dye using Kaolinite Clay and found that the removal efficiency decreased with respect to initial dye concentration due to the elevated collision between the adsorbent and adsorbate (Dadebo and Obura, 2022).


Figure 3: Impact of Dye's initial concentration on the removal efficiency.

3.2.3. Impact of temperature on removal efficiency

The temperature at which the process is conducted also has a mild influence on the performance. If the process requires to be operated at elevated temperatures, then energy expenses will be more and could hinder the scale-up process. For these reasons, a batch-wise study was conducted to study the impact of the temperature and determine the minimum possible temperature where the maximum amount of dye could be adsorbed from the solution. Since it is a batch study, only four different temperatures were adopted to carry out the experiment

and find the corresponding removal efficiency. Hence, the temperature varied from 25 to 40 °C in steps of 5 °C. Other process variables were also set. The amount of dye present before the starting of the experiment was about 75 ppm as it proved to be the best in studies conducted before while the pH was maintained constantly at 7. Also, the dosage level of the adsorbent was fixed at 4 g/L. After the finishing of the experiment which went for around 60 min, the removal efficiency for each batch was carefully evaluated and collated against the temperature. This plot could be found in Figure 4. From the illustration, it could be grasped that the removal efficiency of the biochar slowly increases along with the rise in temperature. This steady growth in trend might be because of the growth in motion of the molecules present due to the breakage of bonds between them. Figure 4 reveals that the peak removal of around 87.640% occurred at 35 °C. Beyond this level, it could be seen that the removal efficiency drops. With that being said, the optimal temperature level of the biochar must be decided for better performance and economics at the same time. Having discussed all these, the removal efficiency of 87.640% at 35 °C grabs our attention. This is the only temperature at which the maximum amount of AR dye could be removed at a relatively lower temperature. The change in percentage of removal from 30 to 35 °C is also promising when compared to others. Hence 35 °C is considered as the best and most efficient temperature. Similarly, Mahendran *et al.* experimented on the effect of temperature on adsorption efficiency on the removal of Reactive Red 120 using biochar derived from *Ulva prolifera* biomass and found that the removal efficiency of the biochar increased with an increase in temperature with the best operating temperature for best removal efficiency being 30 °C (Mahendran *et al.*, 2021).
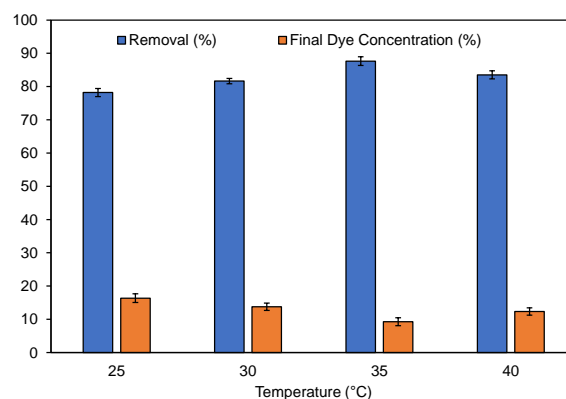
Figure 4. Impact of Temperature on removal efficiency.

3.2.4. Impact of time on removal efficiency

Although very large amounts of contact time don't contribute to the removal efficiency it is always better to determine the optimal amount of time both the dye and biochar should be kept in contact. For these reasons, a batch-wise study was conducted to study the impact of the contact time of AR dye and biochar on the removal of dye in the solution. Since it is a batch study only five different contact periods were adopted to carry out the experiment and find the corresponding removal

efficiency. These periods varied from 30 to 90 min in steps of 15 min. Other process variables were also set. The amount of dye present before the starting of the experiment, the temperature and dosage of biochar were all previous studies and continued to adopt the same for this study. Initially, 75 ppm of dye was present and 4 g/L of biochar was added. After the finishing of the experiment which was held at 35 °C, the removal efficiency for each batch was carefully evaluated and collated against the time. This plot could be found in Figure 5. From the illustration, it could be grasped that the removal efficiency of the biochar slowly increases along with the rise in contact time. A term known as equilibrium adsorption efficiency coined in literature means that the efficacy of any biochar to remove an organic dye always increases until equilibrium is reached [34, 37]. Figure 5 reveals that the peak removal occurred 87.640% occurred at exactly 60 min mark. Beyond this level, it could be seen that the removal efficiency almost holds steady as described by equilibrium adsorption efficiency. With that being said, the optimal contact time of the biochar and dye must be decided for better performance and economics at the same time. Having discussed all these, the removal efficiency of 87.640% at 60 min grabs our attention. This is the only case where more dye could be removed with minimal time. The change in percentage from 45 to 60 min is also promising when compared to others. Hence 60 min of the biochar is considered the best and most efficient contact time. Similar studies were conducted by Dadebo and Obura in which they experimented on the effect of contact time on the removal of Acid Red 88 dye using Kaolinite Clay and found that the removal efficiency increased with respect to contact time up to the point of equilibrium after which there was no increase in removal efficiency with any increase in contact time (Dadebo and Obura, 2022).
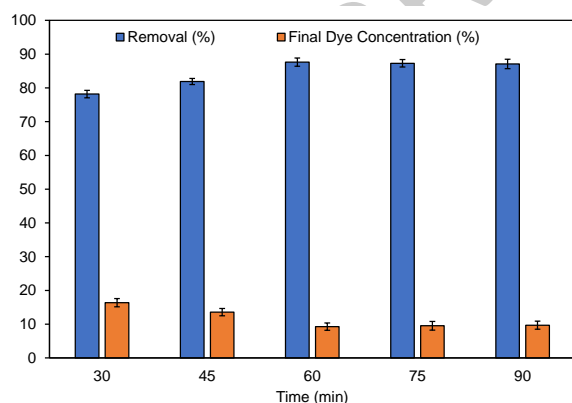

Figure 5: Impact of time on removal efficiency.

3.2.5. Impact of pH on removal efficiency

The acidity and basicity of the solution containing the AR dye molecules could influence the removal efficiency because of the charges present. Hence, a batch-wise study was conducted to study the impact of the pH and evaluate the biochar's capacity to grab the maximum amount of dye solutions with varying pH. Since it is a batch study only seven different pH levels were adopted to carry out the experiment and find the corresponding removal

efficiency. These pH levels varied from 4 to 10 in steps of one. Other process variables were also set. The amount of dye present before the starting of the experiment, contact time, the temperature and dosage of biochar were all previous studies and continued to adopt the same for this study. Initially, 75 ppm of dye was present and 4 g/L of biochar was added. After the finishing of the experiment which was carried out for around 60 min at 35 °C, the removal efficiency for each batch was carefully evaluated and collated against the dosage. This plot could be found in Figure 6. From the illustration, it could be grasped that the removal efficiency of the biochar slowly decreases along with the rise in pH before surging to a peak value of 87.640% at 7 pH and continuing to decline. This steady decline in trend might be because of the populated positive charges on the biochar increasing its potential to adsorb more dye molecules as AR dyes are anionic in nature. Beyond the neutral level, it could be seen that the removal efficiency drops again. Again, beyond 7 pH the biochar begins to acquire negative charges and hence begins to repel the dye molecules leading to a fall in removal. With that being said, the optimal pH level of the solution must be decided for better performance and economical at the same time. Having discussed all these, the removal efficiency of 87.640% at neutral pH grabs our attention. This is possible because the functional groups present in the biochar might be ionized in nature. Hence neutral pH of the solution is considered the best and most efficient pH level. Kumar *et al.* experimented on the adsorption of Reactive Red 120 dye using biochar derived from Ulva reticulata and found that the effect of pH on the adsorption process was similar to that of our study as the Reactive Red 120 dye are also anionic in nature (Kumar et al, 2021).
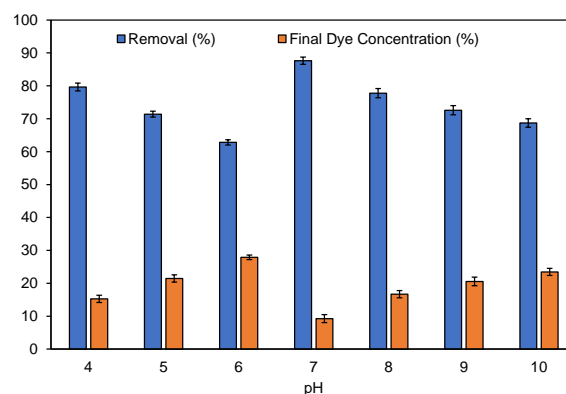

Figure 6: Impact of pH on removal efficiency.

3.3. Isotherm and kinetics study

As mentioned earlier, In this study, Langmuir and Freundlich's isotherm models were employed to model the isotherm data and pseudo-first order, pseudo-second order, Weber-Morris, and Elovich kinetic models were employed to model the kinetics data. The models were fitted to the adsorption experimental data using the MATLAB 2020a software and the obtained results are depicted in the table and graph format. Figure 7 and Table 2 depicts the isotherm plot of the various isotherm model for the batch adsorption experiment and its model parameters respectively. Similarly, Table 3 and Figure 8

depicts the Kinetics model parameters for the batch adsorption experiment and its plot respectively. In general, the best fitting isotherm and kinetics model are analyzed with the help of the correlation coefficient (R^2) value and in this case, from Tables 2 and 3, we can clearly see that the best for isotherm model and kinetics model for this study is the Freundlich isotherm model with Pseudo-second-order kinetics. From the isotherm and kinetics study results, we can conclude that the

adsorption process between the KR derived biochar and the AR dye is via chemisorption mechanism process along with multilayer adsorption onto biochar's uneven adsorption sites. Konicki *et al.* experimented on the adsorption of Acid Red 88 dye using a nanocomposite along with its isotherm and kinetics study, and their adsorption process also followed Freundlich isotherm model with Pseudo-second-order kinetics (Konicki *et al.*, 2017).

Table 2. Isotherm model parameters for this study

| Isotherm Model	SSE	R^2	DFE	Adj. R^2	RMSE
Freundlich	2.3765	0.9812	3	0.9750	0.8900
Langmuir	2.5162	0.9801	3	0.9735	0.9158

SSE – Sum of Error Squared; DFE – Degree of Freedom; RMSE – Room Mean Square Error.

Table 3: Kinetics model parameters for this study

Kinetic model	SSE	R^2	DFE	Adj. R^2	RMSE
Pseudo first order	4.7624	0.9993	4	0.9991	1.0911
Pseudo second order	3.8681	0.9994	4	0.9993	0.9834
Elovich	5.6811	0.9991	4	0.9989	1.1918
Weber-Morris	802.7366	0.8772	4	0.8466	14.1663
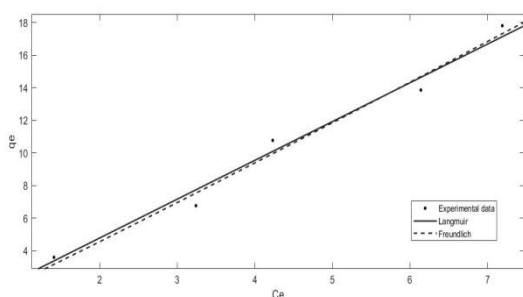
**Figure 7**: Isotherm plot of the Batch Adsorption Experiment.
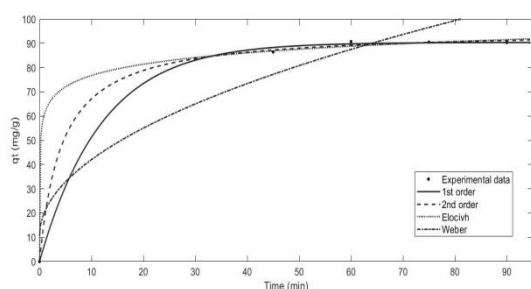
Figure 8: Kinetics plot of the Batch Adsorption Experiment.

3.4. Desorption study

After the intended use of the biochar, it is necessary to find a way to recycle it as much as possible. This not only reduces the expenses but also limits the necessity to produce a vast quantity of biochar from the beginning which demands lots of energy and simply cannot be profitable. Owing to these causes, it is probably better to invest in a recycling technology that could separate most of the adsorbed dye molecules and can be reused without affecting the overall efficiency of the process. To test the capacity of the biochar, the desorption studies were pushed up to four continuous cycles. In this study, NaOH, H_2O and HCl were used as a solvent that could split the biochar and the AR dye molecules. Experiments were

conducted and the results were plotted as shown in Figure 9. As expected, the ability of the elutants to desorb the dye decrease over the course of 4 cycles which is apparent by looking in the figure. Comparing the results of the three elutants, it could be comprehended that NaOH has better desorption ability than the other two with desorption percentages of 84.15, 77.46,62.9 and 55.37. It is already a known notion that when the biochar contains the dye molecules which is negatively charged then it could be easily repelled by other substances that inherently contains a negative charge. Thus, this might be the cause for NaOH to stand out from others which is neutral (H_2O) and acidic (HCl) in nature.
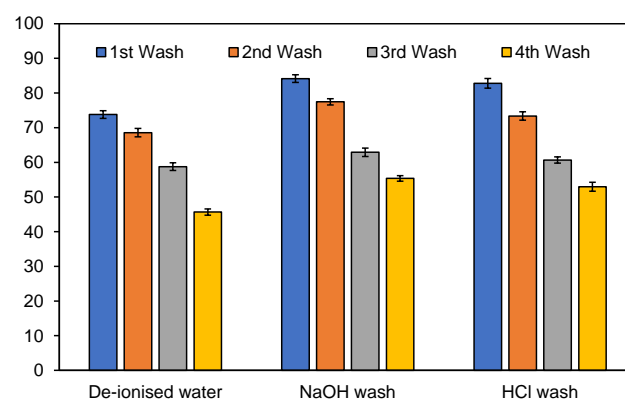

Figure 9: Results of Desorption Studies.

3.5. Column adsorption study

3.5.1. Influence of bead type on the removal efficiency

One of the disadvantages of batch adsorption studies is that it never provides data required for the scaling up procedures. To obtain them we performed column studies where immobilized and adsorption free beads were used to predict and analyze the impact of immobilized chemicals on the adsorption. It came to no surprise that those materials had close to zero effect on the process.

The results of the experiment are represented in Figure 10. On observing the graph, immediately it could be recognized that the encapsulated bead produces far more compromising results than the other two. The peak removal percentages for encapsulated (96.83%) and hybrid beads (87.37%) was achieved at 60 min set. While control beads (26.79%) did decently well in 30 min. In conclusion, the encapsulated beads had a maximum removal of 96.83% and were thus utilized for further studies.
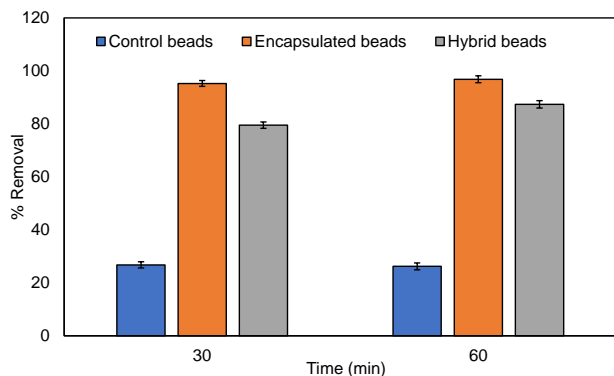
Figure 10: Influence of bead type on the removal efficiency.

3.5.2. Bed-depth service time model

As encapsulated beads were determined to be the efficient ones in the previous studies, they are employed to investigate the dynamic nature of the column by using the BDST model (Bed-depth Service Time). One advantage of using this model is that it could be used to avoid experimental procedures. By using immobilized beads, the model was run by varying the time periods at a fixed flow rate of 15 mL/min and a plot of time versus bed height was plotted. Further, the efficiency of the bed per unit volume denoted by N_o was calculated by taking the slope of the plotted graph shown in Figure 11. The rate constant (k_a) was evaluated by considering the intercept of the graph. By using the rate constant, the rate of transfer of solute between solid and liquid phase was calculated. N_o and K_a was evaluated to be 16.4 mg/mL and 60 L/mg h respectively. Owing to the concentration gradient of metal ions, their capacity to adsorb was greater in the column than in batch study.
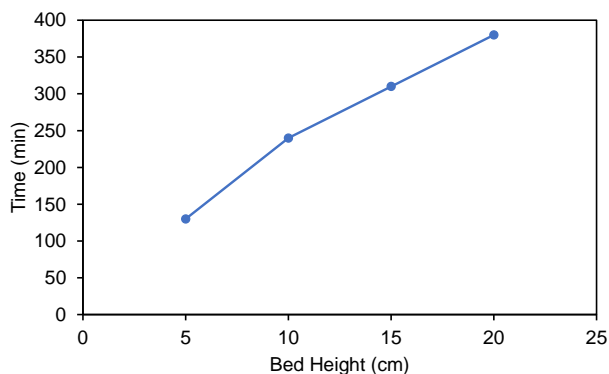
Figure 11: BDST model plot for the removal of AR dye.

4. Conclusion

In the present study, the potential of the *Kappaphycus alvarezii* reject (KR) derived biochar to remove the anionic azo dye, Acid Red 88 from its aqueous solution was studied using batch and column adsorption studies. From the batch adsorption studies, it was revealed that the removal efficiency of the biochar to remove the dye increased with an increase in contact time, biochar dosage, initial dye concentration and temperature but decreased with an increase in pH of the solution due to the anionic nature of the dye. The batch adsorption experiment best fitted to Freundlich isotherm model with Pseudo-second-order kinetics indicating the adsorption to follow chemisorption mechanism process along with multilayer adsorption onto biochar's uneven adsorption sites. The biochar was studied for this desorption efficiency for four consecutive cycles and NaOH proved to be the best elutant for desorption. From this study, we can see that the biochar produced from *Kappaphycus alvarezii* reject has the potential to be utilized as an adsorbent for the efficient removal of anionic dyes. Along with this, this method of utilizing the *Kappaphycus alvarezii* reject will be very economical and beneficial in terms of waste management.

References

Basu P. (2018). Biomass gasification, pyrolysis and torrefaction: practical design and theory, Academic press.

Bhatt D., Shrestha A., Dahal R.K., Acharya B., Basu P., and MacEwen R. (2018). Hydrothermal carbonization of biosolids from waste water treatment plant, *Energies*, **11**, 2286.

Dadebo D., and Obura D. (2022). Removal of Acid Red 88 from an Aqueous Solution Using Kaolinite Clay by Adsorption Process, *East African Journal of Engineering*, **5,** 57–71.

Gokulan R., Avinash A., Prabhu G.G., and Jegan J. (2019). Remediation of remazol dyes by biochar derived from Caulerpa scalpelliformis - An eco-friendly approach, *Journal of Environmental Chemical Engineering*, **7**, 103297. https://doi.org/10.1016/j.jece.2019.103297.

Gokulan R., Ganesh Prabhu G., and Jegan J. (2019). A novel sorbent *Ulva lactuca* -derived biochar for remediation Remazol brilliant orange 3R in packed column, *Water Environment Research*. https://doi.org/10.1002/wer.1092.

Gokulan R., Ganesh Prabhu G., Murugadoss J.R., and Hariharasuthan S. (2018). Optimization of bio-hydrogen production from bio-wastes.

Jayaraju R.M., Gaddam K., Ravindiran G., Palani S., Paulraj M.P., Achuthan A., Saravanan P., and Muniasamy S.K. (2021). Biochar from waste biomass as a biocatalyst for biodiesel production: an overview. *Applied Nanoscience*, **2021**, 1–12. https://doi.org/10.1007/S13204-021-01924-2.

Jegatheesan V., Pramanik B.K., Chen J., Navaratna D., Chang C.-Y., and Shu L. (2016). Treatment of textile wastewater with membrane bioreactor: a critical review, *Bioresource Technology*, **204**, 202–212.

Kalyani G., Gokulan R., and Sujatha S. (2021). Biosorption of zinc metal ion in aqueous solution using biowaste of Pithophora cleveana Wittrock and Mimusops elengi. https://doi.org/10.5004/dwt.2021.27005.

Konicki W., Sibera D., and Narkiewicz U. (2017). Adsorption of Acid Red 88 Anionic Dye from Aqueous Solution onto ZnO/ZnMn2O4 Nanocomposite: Equilibrium, Kinetics, and Thermodynamics, *Polish Journal of Environmental Studies* **26**.

Kumar M., Gokulan R., Sujatha S., Priya S.P.S., Praveen S., and Elayaraja S. (2021). Biodecolorization of Reactive Red 120 in

batch and packed bed column using biochar derived from Ulva reticulata, *Biomass Conversion and Biorefinery*, 1–15.

Li H., Wang S., Yuan X., Xi Y., Huang Z., Tan M., and Li C. (2018). The effects of temperature and color value on hydrochars' properties in hydrothermal carbonization, *Bioresource Technology*, **249,** 574–581.

Mahendran S., Gokulan R., Aravindan A., Rao H.J., Kalyani G., Praveen S., Pushpa T.B., and Senthil Kumar M. (2021). Production of Ulva prolifera derived biochar and evaluation of adsorptive removal of Reactive Red 120: batch, isotherm, kinetic, thermodynamic and regeneration studies, *Biomass Conversion and Biorefinery*, 1–12.

Patel B., Guo M., Izadpanah A., Shah N., and Hellgardt K. (2016). A review on hydrothermal pre-treatment technologies and environmental profiles of algal biomass processing, *Bioresource Technology,* **199**, 288–299.

Patel N., Acharya B., and Basu P. (2021). Hydrothermal Carbonization (HTC) of Seaweed (Macroalgae) for Producing Hydrochar, *Energies*, **14**, 1805.

Praveen S., Gokulan R., Bhagavathi T., and Jegan J. (2021). Techno-economic feasibility of biochar as biosorbent for basic dye sequestration, *Journal of the Indian Chemical Society* **98**, 100107. https://doi.org/ 10.1016/j.jics.2021.100107.

Praveen S., Jegan J., Pushpa T.B., and Gokulan R. (2021). Artificial neural network modelling for biodecolorization of Basic Violet 03 from aqueous solution by biochar derived from agro-bio waste of groundnut hull: Kinetics and thermodynamics, *Chemosphere*, **276**, 130191. https://doi.org/10.1016/J.CHEMOSPHERE.2021.130191.

Ramirez C.H.V. (2017). Biogas production from seaweed biomass: A biorefinery approach.

Rao J., Ravindiran G., Subramanian R., and Saravanan P. (2021). Optimization of process conditions using RSM and ANFIS for the removal of Remazol Brilliant Orange 3R in a packed bed column, *Journal of the Indian Chemical Society*, **98**, 100086. https://doi.org/10.1016/j.jics.2021.100086.

Ravindiran G., Jeyaraju R.M., Josephraj J., and Alagumalai A. (2018). Comparative Desorption Studies on Remediation of Remazol Dyes Using Biochar (Sorbent) Derived from Green Marine Seaweeds, *ChemistrySelect*, **4**. https://doi.org/10.1002/slct.201901348.

Ravindiran G., Saravanan P., Alagumalai A., and Subbarayan S. (2022). Soft computing-based models and decolorization of Reactive Yellow 81 using Ulva Prolifera biochar, *Chemosphere*, **287**, 132368. https://doi.org/10.1016/J.CHEMOSPHERE.2021.132368.

Ravindiran G., Sugumar P., and Elias G. (2021). Continuous Sorption of Remazol Brilliant Orange 3R Using Caulerpa scalpelliformis Biochar, *Advances in Materials Science and Engineering*, **2021**. https://doi.org/10.1155/2021/6397137.

Saravanan P., Thillainayagam B.P., Ravindiran G., and Josephraj J. Evaluation of the adsorption capacity of Cocos Nucifera shell derived biochar for basic dyes sequestration from aqueous solution, https://doi.org/10.1080/15567036.2020.1800142.

Sharma R., Jasrotia K., Singh N., Ghosh P., Srivastava S., Sharma N.R., Singh J., Kanwar R., and Kumar A. (2020). A Comprehensive Review on Hydrothermal Carbonization of Biomass and its Applications, Chemistry Africa, **3**, 1–19. https://doi.org/10.1007/s42250-019-00098-3.

Sivarethinamohan S., Ravindiran G., Hanumanthu J.R., Gaddam K., Saravanan P., and Muniasamy S.K. (2021). Effective removal of remazol brillinat orange 3R using a biochar derived from Ulva reticulata, *Energy Sources, Part A: Recovery, Utilization, and Environmental Effects*, 1–14. https://doi.org/10.1080/15567036.2021.1943070.

Sundar M.L., Kalyani G., Gokulan R., Ragunath S., and Rao H.J. (2021). Comparative adsorptive removal of Reactive Red 120 using RSM and ANFIS models in batch and packed bed column.

Vassilev S.V., Baxter D., Andersen L.K., and Vassileva C.G. (2010). An overview of the chemical composition of biomass, *Fuel*, **89**, 913–933.

Vickers N.J. (2017). Animal communication: when i'm calling you, will you answer too?, *Current Biology, 27*, R713–R715.

Wang T., Zhai Y., Zhu Y., Li C., and Zeng G. (2018). A review of the hydrothermal carbonization of biomass waste for hydrochar formation: Process conditions, fundamentals, and physico-chemical properties, *Renewable & Sustainable Energy Reviews, 90*, 223–247.